STRUCTURE SELECTION IN SYNTHETIC APERTURE RADAR SCATTERING MODELS

Y. Akyildiz and R. L. Moses

Department of Electrical Engineering, The Ohio State University

ABSTRACT

High-frequency models for radar backscatter can include components with different structures that correspond to different physical scattering mechanisms on an object. We consider the problem of structure selection for an attributed scattering center model that includes both localized and distributed scattering terms. We propose three structure classification algorithms, and compare their performance. We show that a threshold test on the estimated length parameter performs as well as a GLRT test, but is computationally more efficient. A computationally fast image-based test is shown to perform as well as the GLRT and length-based tests for scattering center lengths greater than twice the crossrange resolution of the measurements.

1. INTRODUCTION

Synthetic aperture radar (SAR) provides all-weather, day-or-night remote sensing for mapping, search-and-rescue, mine detection, and target recognition [1]. For SAR data processing applications, it is of interest to represent the high-dimensional image data by a low-dimensional model. The low-dimensional model has application in data compression for storage or transmission of SAR data; in addition, the model parameters can serve as features for use in object detection and classification.

We consider an *attributed scattering center* model as a representation of object backscatter in high frequency SAR imagery [3, 4, 6]. The model includes both frequency and aspect dependence, allowing discrimination among a number of scattering primitives. The set of parameters differ for localized and distributed scattering structures. We focus on the structure selection problem. We propose three methods for classifying a scatterer as localized or distributed. The presented techniques are analyzed in terms performance and computational cost.

This work was sponsored by the US Air Force Materiel Command under contract F33615-97-1020. The views and conclusions contained herein are those of the authors and should not be interpreted as necessarily representing the official policies or endorsements, either expressed or implied, of the Air Force Research Laboratory or the U.S. Government.

2. THE PARAMETRIC SCATTERING CENTER MODEL

We adopt a parametric model for the sensor data based on high frequency approximation of electromagnetic scattering [2, 3, 7]. In this model the backscattered electric field from an object can be approximated as the sum of the responses from its electrically isolated scattering centers [4, 6] in additive noise

$$E(f,\phi;\theta) = \sum_{i=1}^{n} E_i(f,\phi;\theta_i) + N(f,\phi) \qquad (1)$$

where $N(f,\phi)$ is assumed to be zero mean Gaussian noise with known covariance, $\theta^T = [\theta_1^T, \ldots, \theta_n^T]$ and

$$E_i(f,\phi;\theta_i) = A_i \exp\left(\frac{-j4\pi f}{c}(x_i\cos\phi + y_i\sin\phi)\right) \cdot \left(j\frac{f}{f_c}\right)^{\alpha_i} g_{k,i}(f,\phi;\theta_i) \qquad (2)$$

The parameters x_i and y_i are the downrange and crossrange locations, A_i is the scattering center amplitude, and $\alpha_i \in [-1, -0.5, 0, 0.5, 1]$ describes the frequency dependence. In addition, $k \in \{\ell, d\}$ distinguishes between a localized or distributed scattering center, with

$$g_{\ell,i}(f,\phi;\theta_{i,\ell}) = \exp(-2\pi f\gamma_i\sin\phi) \qquad (3)$$

$$g_{d,i}(f,\phi,L_i;\theta_{i,d}) = \mathrm{sinc}\left(\frac{2\pi f}{c}L_i\sin(\phi-\bar{\phi}_i)\right) \qquad (4)$$

Thus, $\theta_{i,\ell} = [x_i, y_i, A_i, \alpha_i, \gamma_i]$ and $\theta_{i,d} = [x_i, y_i, A_i, \alpha_i, L_i, \bar{\phi}_i]$. The structure determination problem is to determine whether the ith scattering center is localized or distributed.

The parameters α and $\{\ell, d\}$ distinguish among several scattering geometries. The α parameter relates to the curvature of the scatterer; localized scatterers have energy concentrated near a point in the image, whereas distributed scatterers have energy concentrated along a line segment whose length is approximately L in the SAR image.

2.1. Image Formation and Parameter Estimation

The measured backscatter data is typically collected on a polar segment in the (f,ϕ) plane. The data are resampled to

0-7803-6293-4/00/$10.00 ©2000 IEEE.

a rectilinear grid, windowed, and inverse 2-D Fourier transformed to obtain a complex-valued image $I(x, y)$ on a sampled grid of (x, y) locations. Since the imaging process is linear, the noise $N(x, y)$ in the image domain is also Gaussian with known covariance.

We estimate the parameter vector θ as follows. We exploit the property that the energy of a given scattering center is localized in the image. We segment high energy regions R_k in the image [5], and to each region obtain approximate maximum likelihood (AML) estimates of the parameters of a low-order scattering center model. Because the noise is Gaussian, AML estimates are found by solving a nonlinear minimization problem of the form

$$\begin{aligned} \hat{\theta}_{k,AML} &= \arg\min_{\theta} J(\theta) \\ &= \arg\min_{\theta} [d - s(\theta)]^H \Sigma^{-1} [d - s(\theta)] \end{aligned} \quad (5)$$

where d is a vector of image pixels in the region R_k, $s(\theta)$ is the scattering model vector for these image pixels, and Σ is the covariance matrix of the noise vector for this region. The algorithm is approximate maximum likelihood because we apply the minimization algorithm locally to a subset of the parameters on a subset of the pixels. By estimating model parameters on regions, we decouple the high-order parameter estimation problem into a set of smaller estimation problems, providing a large gain in computational speed with only a slight degradation in estimation performance.

The Cramér-Rao bound (CRB) on estimator variance for the parameters of the attributed scattering center model has been derived [2]. The image-domain nonlinear least squares algorithm has been applied to both synthetic and measured imagery, and is shown to give parameter estimates that are close to the CRB [5].

3. STRUCTURE SELECTION

Each scattering center is described by one of two possible models as shown in equation (2). In this section we address the question of how to choose between the two structures. Previous parameter estimation algorithms [2, 5] either assume the structure is known or estimate the structure from the image segmentation. We propose three different approaches for structure selection: a GLRT approach, a test based on the estimated length, $\hat{L}$ in the distributed model, and a computationally fast image-based approach.

We assume two possible hypotheses for the structure corresponding to a region R_k in the SAR image: either H_ℓ if the scattering center is a single localized response, or H_d if the scattering center is a single distributed response. We define the probability of false alarm P_{FA} as the probability of selecting a distributed scattering center when the true scattering center is localized, and define the probability of detection P_D as the probability of correctly selecting a distributed scattering center. Because the localized and distributed models coincide for $L_i = \gamma_i = 0$, structure selection will be difficult for scattering centers with parameters near these values, even for high SNR.

3.1. GLRT-Based Structure Selection

The GLRT-based test involves computing the AML estimate of the parameter vector θ for an image region under both H_ℓ and H_d, and forming a likelihood ratio test using the estimated parameters; thus:

$$\frac{f(d|H_d, \hat{\theta}_d)}{f(d|H_\ell, \hat{\theta}_\ell)} \underset{H_\ell}{\overset{H_d}{\gtrless}} \eta_{GLRT} \quad (6)$$

Since the noise on d is additive Gaussian, the log-likelihood of d under each hypothesis reduces to a quadratic function given by (to within a constant)

$$\log f(d|H, \hat{\theta}) = \|d - s(\hat{\theta})\|_Q$$

where Q is the inverse of the noise covariance for the vector d.

3.2. $\hat{L}$-Based Structure Selection

In this test we find the parameter vector estimate $\hat{\theta}_d = [\hat{x}, \hat{y}, \hat{A}, \hat{\alpha}, \hat{L}, \hat{\bar{\phi}}]$ that best fits a distributed scattering model for a selected region in the image. The hypothesis test is then given by

$$\hat{L} \underset{H_\ell}{\overset{H_d}{\gtrless}} \eta_L \quad (7)$$

where the threshold η_L is selected by the user.

The decision rule in equation (7) is computationally more attractive than the one in (6) because it avoids estimating $\hat{\theta}_\ell$ under hypothesis H_ℓ.

3.3. Image-Based Structure Selection

A computationally fast structure selection test can be derived by exploiting the shape of the scattering center response in the SAR image. In particular, distributed scattering centers have widths that are larger than the width of a localized scattering center.

The algorithm we propose is as follows. We extract the crossrange pixel samples in the selected region for the downrange distance corresponding to the peak value in the region. This results in a small number of samples (usually between 3–20) $d[k]$ indexed on crossrange location. We then fit a parabola, $ak^2 + bk + c$ to the samples using a least-squares criterion to estimate the parameters (a, b, c). We compute

the 3 dB width $\hat{W}$ of the parabola. The image-based hypothesis test for a localized or distributed scattering center is given by

$$\hat{W} \underset{H_\ell}{\overset{H_d}{\gtrless}} \eta_W \tag{8}$$

where η_W is a user-selectable threshold. The test is computationally very fast, because the parabola coefficients are estimated by solving a system of three linear equations and the 3 dB width is found with simple algebra.

A parabola is chosen because for localized scatterers, the crossrange response is well-approximated by the point spread function of the radar imaging process in the crossrange direction, and for most windows used in radar image formation, this response is well-modeled by a parabola. For a distributed scattering center, the parabola is not as good a fit, but still gives an estimate $\hat{W}$ which is above any threshold η_W chosen for practical false alarm probabilities (see Section 4). In addition, the parabola gives a real-valued estimate of $\hat{W}$ (not quantized by pixel samples); this gives robustness to the center location (x_i, y_i) of the scattering center.

4. NUMERICAL RESULTS

In this section we evaluate the performance of the three proposed structure detection tests presented in the previous section.

Figure 1 shows the difference in fit error when a distributed and a localized model are used to model a distributed scattering center with true length L_c, measured in crossrange resolution units. For each value of L_c we generate 20 realizations of the scattering center with different center locations (x and y) to account for estimation differences as a function of location. For each realization we obtain a data vector d in the high-energy region, estimate $\hat{\theta}_\ell$ from d, and form the reconstructed image pixel vector $s(\theta_\ell)$. We compute the normalized difference $\|s(\theta_\ell) - d\|/\|d\|$, where d is the vector of pixels corresponding to the true model. We also compute $\|n\|/\|d\|$, where n is a vector of noise pixels corresponding to a scattering center with SNR of 20 dB. Here, SNR is defined as the ratio of the peak amplitude of the scattering center to the noise standard deviation in the image domain. We plot the minimum, mean, and maximum of these norm ratios for several values of L_c. We expect to be able to discriminate a localized from a distributed scattering center only when the differences in the model norms become greater than the noise component of the norm. As seen in Figure 1, for a signal-to-noise ratio of 20 dB, an L_c value greater than 1.8 is required to reliably detect a distributed scatterer.

Figure 2 shows P_D versus P_{FA} for SNR=20 dB and for the three structure hypothesis tests proposed in Section 4. The GLRT and the $\hat{L}$ tests perform nearly identically for all values of L_c; we thus prefer the $\hat{L}$ for structure selection because it has lower computational cost than the GLRT.

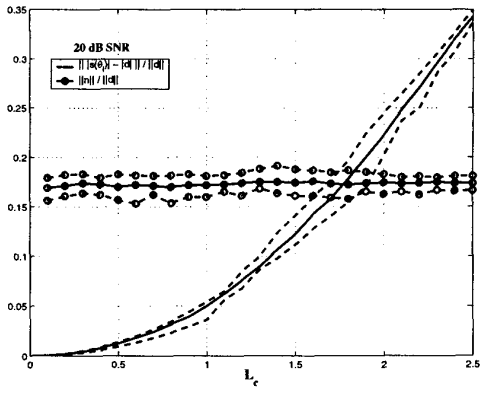

Figure 1: Normalized error norm between localized and distributed scattering model for a distributed scattering center with length L_c. Also displayed is the normalized norm of the noise component for 20 dB SNR value. The minimum, mean, and maximum norm for 20 realizations are shown.

All three tests perform similarly, and not much better than chance, for $L_c \leq 0.5$; this is consistent with predictions based on Figure 1. For $L_c \in [0.5, 2]$ times the crossrange resolution, the the GLRT and $\hat{L}$ tests perform significantly better than the image-based test. For $L_c \geq 2$, all three tests give very few errors in structure selection. The critical values of $L_c = 0.5$ and $L_c = 2$ change only slightly as SNR changes, but otherwise the above comments apply for other SNR values as well. Thus, one can use the computationally fast image-based test to discriminate between scattering center structures if the distributed scattering centers have greater than about two times the crossrange resolution.

5. CONCLUSIONS

We have presented three methods for structure detection of a scattering center using the attributed scattering center model in [3]: a GLRT-based test, a simpler test based on the scatterer length estimate assuming a nonzero-length scattering center, and a computationally fast test based on the width of the scattering center line segment in the image plane. The computationally less expensive length-based test gives the same detection performance as the GLRT test for all scattering center lengths. None of the structure detectors was effective for scattering center lengths below about 0.5 times the SAR image crossrange resolution. For lengths greater than about two times the crossrange resolution, all three structure selection algorithms were able to almost perfectly select the correct model structure. The GLRT and the $\hat{L}$ tests perform nearly identically, and have better performance than the computationally much faster image-based test only for distributed scattering center lengths in the range of 0.5–2

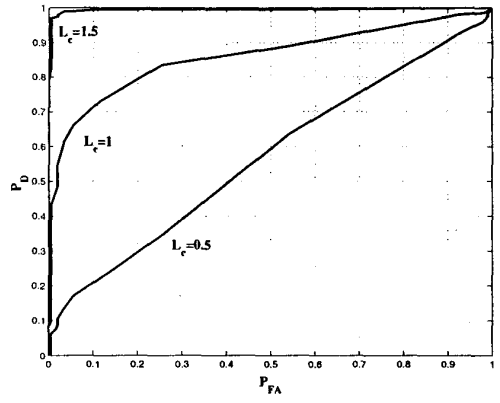

(a) GLRT test

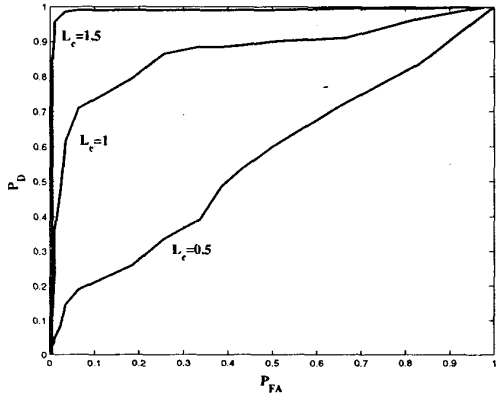

(b) $\hat{L}$ test

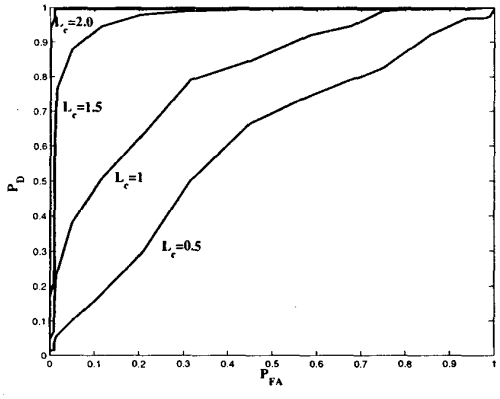

(c) Image-based test

Figure 2: Detection versus false alarm probabilities of the three proposed structure selection algorithms

times the crossrange resolution. The price paid for the increased performance is increased computation to implement these tests.

6. REFERENCES

[1] Curlander C., and McDonough R. N., *Synthetic aperture radar: systems and signal processing*, Wiley, New York, 1991.

[2] Gerry M. J., *Two-dimensional Inverse Scattering Based on the GTD Model.* PhD Dissertation, The Ohio State University, Columbus, OH, 1997.

[3] Gerry M. J., Potter L. C., Gupta I. J., and van der Merwe A., "A parametric model for synthetic aperture radar measurements," *IEEE Trans. Antennas and Propagation* **47**, July 1999.

[4] Keller J. B., "Geometrical theory of diffraction," *J. Opt. Soc. Am.* **52**(2), pp. 116–130, 1962.

[5] Koets M. A., and Moses R. L., "Feature Extraction using Attributed Scattering Center Models on SAR Imagery," in *SPIE*, (Orlando, Florida), April 1999.

[6] Kouyoumjian R. G., and Pathak P. H., "A uniform geometrical theory of diffracti for an edge in a perfectly conducting surface," *Proc. IEEE* **62**, pp. 1448–1461, November 1974.

[7] Potter L. C., and Moses R. L., "Attributed scattering centers for SAR ATR," *IEEE Trans. Image Processing* **6**, pp. 79–91, January 1997.